Structural Engineering and Mechanics, *Vol. 65, No. 4 (2018) 477-490*
DOI: https://doi.org/10.12989/sem.2018.65.4.477

Strengthening of preloaded RC columns by post compressed plates-a review

L. Wang[1] and R.K.L. Su*[2]

[1]*College of Civil Engineering, Nanjing Tech University, China*
[2]*Department of Civil Engineering, The University of Hong Kong, Hong Kong, China*

(Received August 14, 2017, Revised December 11, 2017, Accepted December 12, 2017)

Abstract. Reinforced concrete (RC) columns, as the primary load-bearing structural components in buildings, may need to be strengthened due to material deteriorations, changes in usage, new building codes or new design requirements. The use of post compressed plates (PCP) to strengthen existing RC columns has been proven experimentally and practically to be effective in solving stress-lagging effects between the original column and the new strengthening jacket caused by the pre-existing loads. This paper presents a comprehensive summary and review of PCP strengthening techniques to strengthen preloaded RC columns. The failure mode, deformability, and ductility of the strengthened RC columns are reviewed.

Keywords: RC columns; strengthening; preloaded; post compressed plates; ultimate load capacity

1. Introduction

Along with time passing, a large number of old buildings need to be retrofitted or repaired in the world, especially in East Asian, where has been transformed to world economic center. The aging and degradation of reinforced concrete (RC) has created serious structural problems. Simply dismantling the old buildings that are not up to current design standards or do not fit for their current usage is environmentally unfriendly, unsustainable and sometimes uneconomical. The construction waste generated would impose a huge demand on additional landfill space, which could significantly shorten the life-span of existing landfill sites. Furthermore, many old and historic buildings encapsulate the collective memory of the people. Many people, in particular the elderly, are often reluctant to move out from their old home. To conserve the social, cultural and historical value and the collective memory of the buildings as well as to rehabilitate the degraded structures, many old buildings have to be preserved and upgraded.

Many reinforced concrete structural components, especially the concrete columns, are key load-bearing structural components in buildings. Lots of them may need to be strengthened due to defective construction, having higher loads than those foreseen in the initial design of the structure, or as a result of material deterioration or accidental damage. To upgrade existing RC columns, external jacketing is often used since it is recognized as one of the most convenient way to strengthen existing RC columns. Up to now, three principal jacketing are available for column strengthening: concrete jacketing, steel jacketing and composite jacketing using FRP (Wu *et al*. 2006, Teng *et al*. 2003, Achillopoulou and Karabinis 2013, Harajli *et al*. 2006, Yuce *et al*. 2007, Pellegrino and Modena 2010, Elwan and Rashed 2011, Fukuyama and Sugano 2000, Cirtek 2001, Ramirez 1996, Frangou *et al*. 1995, Giménez *et al*. 2009a, Zhang *et al*. 2015, Kumar and Petel 2000). With these methods, jackets are placed around the columns to increase the sectional area and/or confinement of the concrete so as to directly or indirectly increase the axial load capacity of the columns.

Although the use of jackets has become a common practice worldwide, there are still some unresolved issues regarding the effects of stress lagging between the original concrete core and the jackets (Giménez *et al*. 2009b, Ersoy *et al*. 1993, Takeuti *et al*. 2008) and the difficulty of providing uniform confinement around rectangular cross sections (Wu *et al*. 2006, Wu and Wei 2010). To address these issues, a simple and innovative post compressed plates (PCP) strengthening technique was proposed to strengthen preloaded RC columns by Su and Wang (2009). In this approach, slightly precambered steel plates are bolted to the RC member, as shown in Fig. 1(a). As the plates provided are longer than the clear height of the column, progressive tightening the anchor bolts can generate a thrust on the beam supports by means of arching actions. Unlike other strengthening methods, the present approach can actively share the existing axial loads in the original column with additional steel plates. The stress relief in the original column and post-stress developed in the steel plates could alleviate the stress lagging and displacement incompatibility problems. As similar strains are induced in the RC column and steel plates, a better utilization of both components in resisting external load, and hence a higher axial load-carrying capacity, can be achieved.

The theory of this strengthening method is similar to the principle of pre-stressed concrete. The amount of post-compressed plate forces induced is controlled by the initial precamber displacement of the steel plates. By applying this

*Corresponding author, Ph.D.
E-mail: klsu@hku.hk

http://www.techno-press.com/journals/sem&subpage=7
ISSN: 1225-4568 (Print), 1598-6217 (Online)

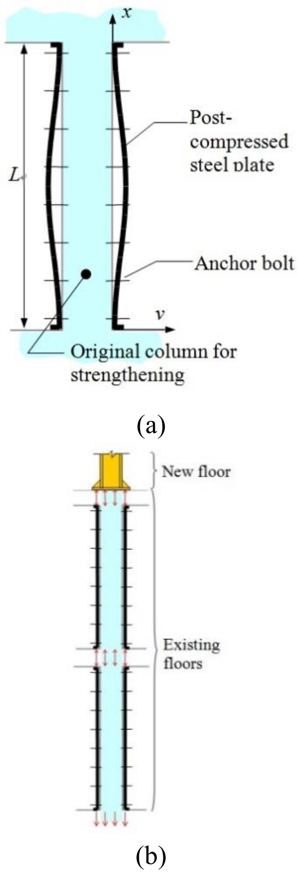

Fig. 1 Illustration of column strengthening by post-compression plate: (a) single storey and (b) multiple storeys

strengthening method in each floor successively, the additional loads can be transferred down to the foundation, as shown in Fig. 1(b).

In this paper, the experimental and analytical studies conducted on preloaded RC columns strengthened with PCP are reviewed. The axial strengthening of RC columns is discussed in Section 2. This is followed by the discussions on RC columns strengthened with PCP under small and large eccentric compressive loading in Section 3 and Section 4, respectively. In Section 5, the fire damaged RC columns strengthened with PCP is discussed. The corresponding analytical models are presented, which allow post compressed plate strengthened RC columns to be designed with confidence.

2. Axial strengthening of RC columns

2.1 General

Existing RC columns can be strengthened with externally pasted steel jacketing. When compared with other strengthening schemes, the use of steel jacketing can maintain the ductility of columns. However, the researches on the effects of pre-existing loads on stress-lagging between the concrete core and the new jacket are still very little. Some test results show a 50% reduction in the ultimate load capacity of the preloaded column.

To address the mentioned issues, the post-compressed approach was proposed to strengthen preloaded RC rectangular columns under axial compression by Su and Wang (2009). They conducted experimental and analytical studies to prove that this strengthening method could greatly increase the axial load capacity and deformability of RC columns. Furthermore, the corresponding theoretical model for predicting the ultimate load capacity of strengthened columns was also proposed.

2.2 Post stressed procedure

One of the key steps in this strengthening method is to decompress the RC column by flattening the precambered plates. A major difficulty is that the steel plates could be warped (buckled) if the post stressed procedure is not conducted properly. To overcome this difficulty, a unified post stressed procedure was proposed by Su and Wang (2012), as shown in Fig. 2. In order to increase the critical buckling load of plates and to avoid warping effects, precambered plates were pressed to form high-order buckling modes, instead of a first-order buckling mode, during the post-stress procedure. The process can be divided into the following three steps: (i) bolts at the mid-height are tightened as shown in Fig. 2(b); thus, the buckling mode of the precambered plate is changed to higher modes, (ii) the plates are flattened by tightening the other bolts as shown in Fig. 2(c) and (iii) to achieve a more evenly distributed internal stress in the plates, all the bolts are slightly loosened and fastened again as shown in Figs. 2(d) and (e).

2.3 Experimental observations

A detailed experimental study (Su and Wang, 2012 and Wang 2013) was carried out to validate the effectiveness of PCP strengthening method. Fifteen specimens were fabricated and tested. The RC cross section is 100 mm × 150 mm, and the clear heights of the columns are 600 mm (Specimens SC1 to SC10) and 1200 mm (Specimens HSC1 to HSC5), respectively. For all specimens, a vertical reinforcement of 4T10 is arranged and a transverse reinforcement of R6-80 is applied along the height of the column. Specimens SC1 and HSC1 are control specimens without any strengthening measure. Specimens SC2 and HSC2 are strengthened using flat steel plates and are not subjected to preloading before strengthening. Therefore, they do not have any stress-lagging problem. Specimen SC3 is plate-strengthened by the same steel plate arrangement as Specimen SC2, except that it is preloaded (P_{pl} = 275 kN) before strengthening. Comparing the performances of Specimens SC2 and SC3 reveals the effects of stress-lagging on the axial load capacity. The other specimens are strengthened by post-compressed steel plates with varying initial precamber (δ), thickness (t_{pc}) and preloading (P_{pl}). The design parameters and preloads for all specimens are provided in Table 1.

In order to control the initial precamber for PCP strengthened columns, stainless steel rods with a diameter equal to the required initial precamber are inserted between the concrete and steel plates at the middle height of the

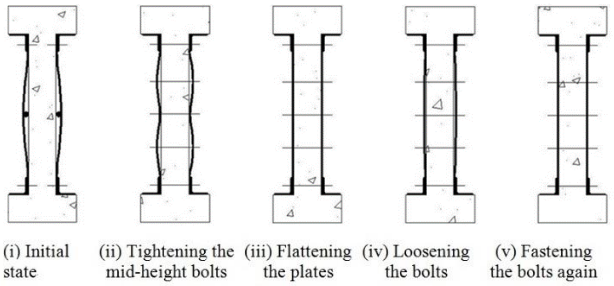

Fig. 2 Post-stressed procedure for columns under axial compression

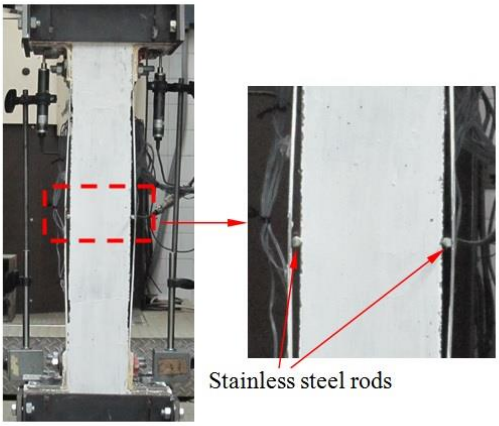

(a)

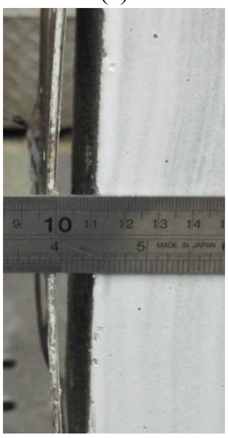

(b)

Fig. 3 Initial precamber of Specimen SC6: (a) stainless steel rods and (b) 10 mm initial precamber

column, as shown in Fig. 3(a). The bolts at both ends of the column are then tightened to form the desired initial precamber profile, as shown in Fig. 3(b). The gaps between the steel angles and the concrete at the base and top of the steel plates are filled with an injection plaster, forming a layer of bedding between the steel angles and the concrete. The steel plates were fixed by Grade 8.8 bolts of diameter 12 mm.

Table 1 summarizes the axial load capacities of all the specimens. For the columns with 600 mm height, all the plate-strengthened columns show a significant improvement in axial strength, from 12.8% to 75.0%, when compared with the control specimen (SC1). Among the seven

Table 1 Summary of strengthening details and test results of specimens under axial loading

Specimen	f_{cu} (MPa)	t_{pc} (mm)	δ (mm)	P_{pl} (kN)	γ	P_{exp} (kN)	P_{pre} (kN)	P_{pre}/P_{exp}
SC1	31.3	-	-	-	-	549	459	0.84
SC2	28.6	6	0	0	1	961	949	0.99
SC3	28.6	6	0	275	0.57	675	699	1.04
SC4	31.2	3	6	275	0.71	619	575	0.93
SC5	31.2	3	10	275	0.82	647	609	0.94
SC6	28.3	3	10	165	1	736	658	0.89
SC7	28.8	6	6	275	0.68	833	761	0.91
SC8	28.5	6	10	275	0.84	897	848	0.95
SC9	30.3	6	6	385	0.36	633	595	0.94
SC10	32.2	6	10	385	0.64	836	772	0.92
HSC1	29.6	-	-	-	-	531	442	0.83
HSC2	28.7	3	0	0	1	701	662	0.94
HSC3	28	3	20	275	0.64	575	537	0.93
HSC4	28.3	6	12	275	0.58	733	677	0.92
HSC5	27.3	6	20	275	0.69	739	729	0.99

* f_{cu} = the concrete cube compression strength on the 28th day; t_{pc} = the thickness of a steel plate; δ = the initial precamber; P_{pl} = the preloading level; γ =the plate strength utilization coefficient; P_{exp} = the experimental ultimate load capacity; P_{pre} = the predicted ultimate load capacity

specimens strengthened with post-compressed plates, the ultimate capacities of Specimens SC4 to SC10 increase by 12.8%, 17.9%, 34.1%, 51.7%, 63.4%, 14.4% and 52.3%, respectively. For the columns with 1200 mm height, the ultimate capacities of Specimens HSC2 to HSC5 increase by 32.0%, 8.3%, 38.0% and 39.2%, respectively, when compared with the control column (HSC1). It should be noted that the ultimate load capacity of Specimen SC3 is slightly less than expected because bedding at the top of the steel angles is packed unevenly and the plates could not reach their full resistance. The standard of workmanship on packing is improved for other specimens and similar errors are prevented.

The concrete crack patterns of the test specimens are quite similar. Cracks usually occur at the mid-height of the columns and then propagate in the vertical direction. As the applied load is increased, major cracks are extended and inclined cracks are formed. Adding steel plates delays the occurrence of the first crack in the concrete. Furthermore, cracks form later when thicker steel plates are used. Figs. 4(a), (d) and (i) show the crack patterns of Specimen SC4, Specimen SC6 and Specimen HSC5, respectively.

From the strain gauges attached to the longitudinal reinforcements and steel plates, the strains and internal stresses are calculated. The strain data indicates that once concrete crushing occurred, the steel plates reach their yield strength rapidly because the compressive load that is originally resisted by the concrete is transferred to the steel plates. Plate buckling is suppressed by providing closely spaced bolts; therefore, it does not occur prior to concrete

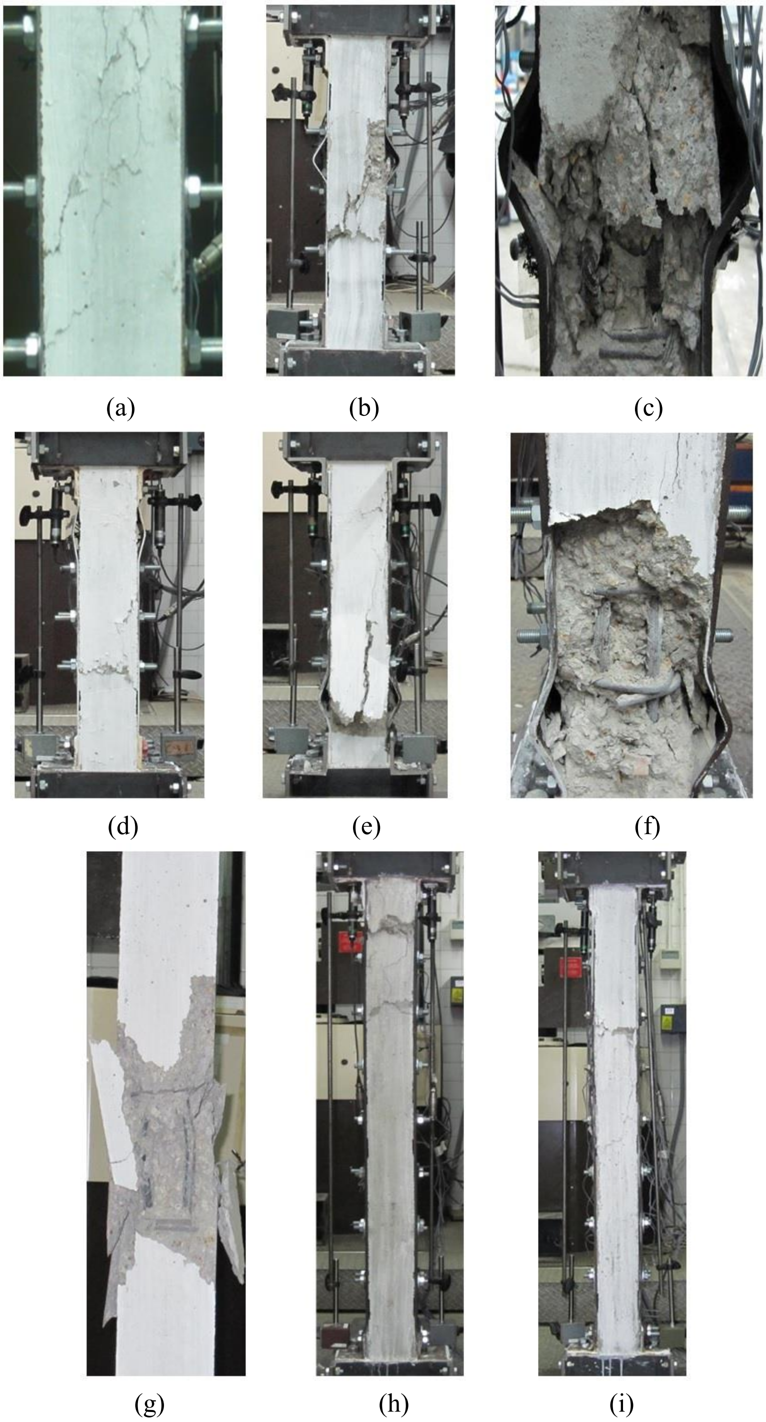

Fig. 4 Crack patterns: (a) Specimen SC4; (b) Specimen SC5 front view; (c) Specimen SC5 rear view; (d) Specimen SC6; (e) Specimen SC9 front view; (f) Specimen SC9 rear view; (g) Specimen HSC1; (h) Specimen HSC4 and (i) Specimen HSC5

crushing.

All failure modes of the plate-strengthened columns are associated with concrete crushing except for Specimens SC2 and SC6, as shown in Figs. 4(b), (c), (e), (f), (g) and (h). These results are expected because yielding of plates prior to concrete failure is a design specification. Assuming there is no bond slippage between the longitudinal bars and the concrete before failure, the strains measured in the steel bars are the same as that of the concrete. The strain gauge readings reveal that the steel plates and concrete of SC6 reach their peak capacities almost simultaneously. The failure of this Specimen SC2 is initiated by steel plate yielding prior to concrete crushing. Specimen SC2 is not subjected to any preloading before strengthening; therefore, these results indicate that without preloading, steel plates can reach their yield strength before concrete crushing occurs.

2.4 Estimation of ultimate axial load capacity

Owing to the fact that bolts at both ends of the steel

Table 2 Summary of strengthening details of specimens under small eccentric loading

Group	Specimen	f_{cu} (MPa)	f_c' (MPa)	e (mm)	t_{pc} (mm)	δ (mm)	P_{pl} (kN)
[A]	ESC1-1	31.3	25.6	30	-	-	-
	ESC1-2	31.9	25.8	30	3	10	101
	ESC1-3	32.6	25.9	30	6	10	101
	ESC1-4	32.7	26.1	30	6	6	101
[B]	ESC2-1	33.3	27.8	70	-	-	-
	ESC2-2	32	25.7	70	3	10	63
	ESC2-3	32.2	25.9	70	6	10	63

* f_c '= the concrete cylinder compression strength on the 28th day; e = the eccentricity

plates restrain the end rotations of plates, the initial lateral displacement (v) of the precambered plate can be approximated by a cosine function (Su and Wang 2009) as expressed

$$v=\frac{\delta}{2}\left(1-\cos\left(\frac{2\pi x}{L_{rc,pl}}\right)\right) \tag{1}$$

where δ is the initial precamber at the mid-height of the plate, $L_{rc,pl}$ is the clear height of the RC column under preloading (N_{pl}), x is the coordinate defined along the height of the column, and the subscript pl denotes the preloading stage. Eq. (1) satisfies the boundary conditions at both ends of the steel plates, i.e., $v=0$ and $\frac{dv}{dx}=0$ when x=0 or $x=L_{rc,pl}$.

According to force equilibrium and compatibility conditions, the analytical ultimate axial load capacity of plate-strengthened RC columns can be expressed as (Su and Wang 2012)

$$N_{prc}=0.67A_c f_{cu}+A_s f_{sy}+2\gamma A_p f_{py} \tag{2}$$

where f_{cu}, f_{sy} and f_{py} are the concrete cube compressive strength, yield strength of steel bars and yield strength of steel plates, respectively. A_c, A_s and A_p are cross-sectional areas of the RC column, vertical steel bars and a steel plate, respectively. γ is defined as plate strength utilisation coefficient, which is expressed as (Su and Wang 2012)

$$\gamma=\begin{cases}\dfrac{E_p\varepsilon_{c0}(-5E_sA_s\varepsilon_{c0}+\sqrt{A_cf_{cu}(64A_cf_{cu}+80E_sA_s\varepsilon_{c0}+160E_pA_p\varepsilon_{p,ps}-80N_{pl})+25E_s^2A_s^2\varepsilon_{c0}^2})}{8A_cf_{cu}f_{py}} & (\varepsilon_p<\varepsilon_{py}) \\ 1 & (\varepsilon_p\geq\varepsilon_{py})\end{cases} \tag{3}$$

where E_s and E_p are Young's modulus of steel bar and plate, respectively. ε_{co} is the concrete compressive strain corresponding to f_c', which is the concrete cylinder compressive strength, usually equal to 0.8 of the concrete cube compressive strength (f_{cu}). $\varepsilon_{p,ps}$ is the axial strain in the steel plates in the post-stressing stage. ε_{py} is yield strain of steel plate.

The coefficient 0.67 which was proposed by Kong *et al*. (1987) is used to account for a number of factors involving the height-to-width ratio of the RC column, the loading rate and the compaction of concrete. This value has been widely adopted by various researchers; for instance, by Park and Paulay (1975).

If the local buckling of steel plates occurs before the plate-strengthened column reaches its ultimate load capacity, then the critical load of the steel plate ($N_{p,cr}$) can be calculated by the Euler buckling equation (Timoshenko and Gere 1961).

$$N_{p,cr}=\frac{\pi^2E_pI_p}{(\mu s_{\max})^2} \tag{4}$$

where s_{max} is the maximum bolt spacing and μ a factor related to the boundary conditions for the columns. In the present case, as both ends of the steel plates are clamped, μ is equal to 0.5.

To prevent local buckling of the steel plates, the plate buckling load should be higher than the designed axial force in the steel plate. Hence,

$$N_{p,cr}>\gamma A_pf_{py} \tag{5}$$

The maximum bolt spacing for preventing local plate buckling can be determined by using Eqs. (4) and (5).

The plate strength utilization coefficient (γ) and the predicted axial load capacity (P_{pre}) of the specimens are presented in Table 1. The coefficient (γ) of two specimens (SC2 and SC6) reach unity; this means that the plate strength is fully utilized and that yielding of the plates is expected during the failure of the specimens. Comparing the analytical and experimental axial load capacities reveals that the proposed design procedure is generally able to conservatively estimate the actual axial load capacities of the PCP strengthened columns with an average underestimation of 7%.

3. Strengthening of RC columns under small eccentric compression loading

3.1 General

In this section, an experimental study on RC columns strengthened with post-compressed steel plates under small eccentric compression loading is undertaken. Ten RC columns with different eccentricities, plate thicknesses and initial precamber displacements are tested, and the steel plates are installed on both side faces of RC columns, as shown in Fig. 5. According to the degrees of eccentricity, specimens are divided into two groups. In each group, one column without strengthening is tested to act as a control specimen, while the others are strengthened by post-compressed steel plates. The test results and the associated data analysis of the experimental study are reported. The strength, deformability and ductility performance of PCP strengthened columns are first evaluated and then the effects of steel plate thickness, initial precamber displacements and preloading level on the ultimate load capacity of PCP strengthened columns are given.

In the past ten years, some analytical models used to predict load-carrying capacity of the eccentrically strengthened columns have been proposed. Montuori and

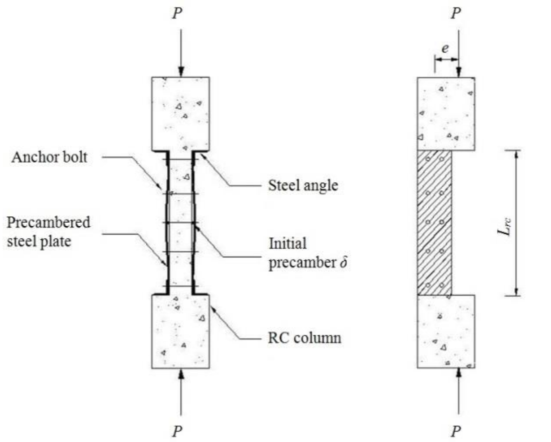

Fig. 5 The configuration of the column decompression approach

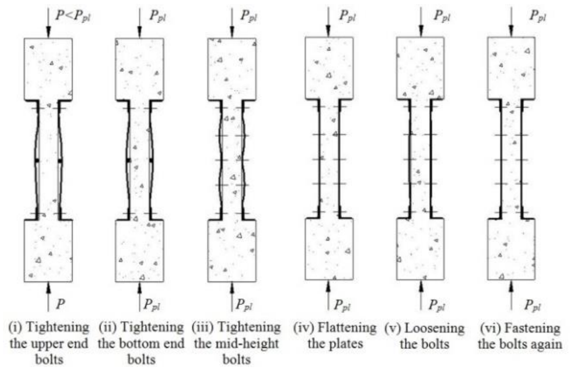

Fig. 6 Post-stressed procedure for columns under small eccentric compression

Piluso (2009) proposed a theoretical model that is able to predict the load-carrying capacity of the strengthened columns based on a kinematic mechanism. Eurocode No. 4 also gives the equations to calculate the ultimate load capacity and bending strength of composite columns under eccentric compression loading. However, the stress-lagging effects on the load-carrying capacity of the strengthened columns have not considered in these models.

According to the aforementioned shortcoming, an original theoretical model with consideration of stress-lagging effects is developed to predict the ultimate load capacity of PCP strengthened columns under eccentric compression loading in this chapter. The accuracy of the model is verified through a comparison of the predicted results with experimental results.

3.2 Post pressed procedure

Wang and Su (2012a) proposed a unified post-stress procedure is shown in Fig. 6. The process can be divided into the following steps: (i) bolts at the upper end of columns are tightened while the others are loosened before reaching the preloading level; (ii) bolts at the both ends of columns are tightened when the specimen under preloading level, meanwhile the gaps between concrete and steel plates are filled with plaster until it reaches the hardening time; (iii) bolts at the mid-height are tightened, and, thus, the buckling mode of the post-compressed plate is changed to higher modes; and (iv) the plates are flattened by tightening the rest of the bolts and (v & vi) to achieve a more evenly distributed internal stress in the plates, and all of the bolts are slightly loosened and fastened again.

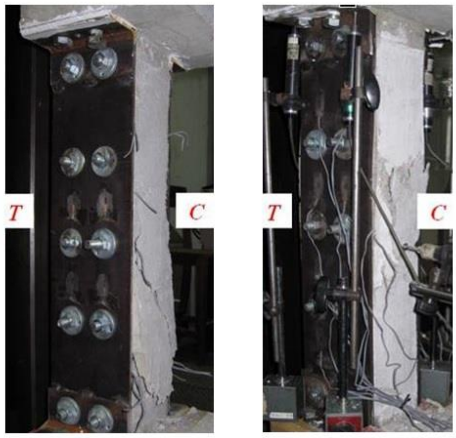

**T* denotes the tension side, *C* denotes the compression side.

Fig. 7 Crack patterns: (a) Specimen ESC1-3 and (b) Specimen ESC2-3

3.3 Experimental observations

All specimens have the same dimensions with a clear column height (L_{rc}) of 600 mm and a uniform cross section of 150 mm × 100 mm. The 4T10 vertical steel bars are arranged, and a transverse reinforcement of R6 is applied along the height of the column. To prevent local failure, both ends of the specimen are enlarged and heavily reinforced. The design parameters, the preload and the compressive strength of the concrete cylinder ($f_c^{'}$) for all specimens are summarized in Table 2.

The concrete crack patterns of the test specimens in each group is quite similar. For the specimens in Group A and Group B, the initial concrete cracks usually occur at the mid-height of the columns on the compression side and then propagate in the vertical direction. With an increasing applied load, the major cracks are extended and concrete is spalled, as shown in Figs. 7(a) and (b). The addition of steel plates delays the occurrence of the first crack in the concrete.

Compared with the control column in each of the groups, the strengthened specimens show various degrees of strengthening from 10.5% to 64.0%, which are summarised in Table 3. In Group A, the ultimate load capacities of Specimens ESC1-2, ESC1-3 and ESC1-4 are increased by 27.1%, 64.0% and 44.6%, respectively. In Group B, the ultimate load capacities of Specimens ESC2-2 and Specimen ESC2-3 are enhanced by 13.9% and 23.9%, respectively.

Due to the eccentricity of the applied axial load, a bending moment is always generated. The ultimate moment (M_u) at the mid-height of the column is composed of the primary moment (M_p) calculated based on the nominal eccentricity and the secondary moment (M_s) caused by the

Table 3 Summary of test results of specimens under small eccentric loading

Group	Specimen	λ	η	P_{exp} (kN)	P_{pre} (kN)	P_{pre}/P_{exp}
[A]	ESC1-1	1.32	1.37	336	329	0.98
	ESC1-2	1.68	1.41	427	390	0.91
	ESC1-3	2.13	1.84	551	545	0.99
	ESC1-4	2.19	1.78	486	471	0.97
[B]	ESC2-1	1.29	1.36	209	208	1
	ESC2-2	1.7	1.43	238	227	0.95
	ESC2-3	2.75	1.87	259	280	1.08

*λ= the deformability factor; η= the displacement ductility factor

P-Δ effect (Wang and Su 2012b), which are summarized in Table 3. The primary, secondary and ultimate moments are defined as follows

$$M_p = P \times e \tag{6}$$

$$M_s = P \times \zeta_u \tag{7}$$

$$M_u = M_p + M_s \tag{8}$$

where P is the applied axial load and ζ_u, which is read from the LVDT at the mid-height of the column, is the lateral mid-height deflection at the ultimate load. For the control columns, the secondary moment due to the P-Δ effect varied from 9.2% to 15.5%. For the strengthened columns with 6-mm-thick plates, the secondary moment varies from 14.3% to 18.3%, while, for the strengthened columns with 3-mm-thick plates, it varies from 9.3% to 15.6%.

3.4 Deformation and ductility

The deformability factor (λ) defined in Eq. (9) and displacement ductility factor (η) defined in Eq. (10) are adopted to evaluate the deformation and ductility performances of the strengthened columns.

$$\lambda = \Delta_f / \Delta_u \tag{9}$$

$$\eta = \Delta_u / \Delta_y \tag{10}$$

The experimental results (Wang and Su 2012) indicate that the plate thickness plays an important role in increasing the deformability and ductility of the strengthened columns, whereas the initial precamber and eccentricity do not have a substantial effect on the displacement ductility of columns. In the meantime, the displacement ductility is also not sensitive to the eccentricity of the applied load.

3.5 Estimation of ultimate load capacity

According to the equilibrium equations obtained from the sum of the internal forces and from taking moments about the tension steel, the ultimate load capacity of strengthened RC columns can be calculated by Eqs. (11) and (12) (Wang and Su 2012b)

$$P_{pre} = \alpha\beta b(c_u - 2d_b) f_c^{'} + A_{sc} f_{scy} - A_{st} f_{st} + 2P_{pcu} - 2P_{ptu} \tag{11}$$

$$P_{pre}e' = \alpha\beta b(c_u - 2d_b) f_c^{'}(d - \frac{\beta c_u}{2}) + A_{sc} f_{scy}(d - d^{'}) + 2P_{pcu}d_{pcu} - 2P_{ptu}d_{ptu} \tag{12}$$

where f_{scy} is the compression steel yield strength, f_{st} is the stress in the tension steel, P_{pcu} and P_{ptu} are the forces calculated by Eqs. (13) and (16), and d_{pcu} and d_{ptu} are the distances from the center of force P_{pcu} and force P_{ptu} to the tension steel, respectively.

Force P_{pcu} at the ultimate load is

$$P_{pcu} = t_{pc} f_{py} h \tag{13}$$

where t_p is the thickness of plate, f_{py} is the yield strength of steel plate, and c_{pu} is the depth of the neutral axis measured from the extreme compression fiber of the steel plate, which can be calculated by

$$c_{pu} = \begin{cases} h & (\text{Case1, } c_{pu} \geq h) \\ (\varepsilon_{cu} - \varepsilon_{c,ps} + \varepsilon_{pc,ps})/\phi & (\text{Case2, } c_{pu} < h) \end{cases} \tag{14}$$

where h is the width of steel plate and ϕ is the change of curvature of RC column between the post-stressing stage and the ultimate load stage, which can be expressed as

$$\phi = \phi_u - \phi_{ps} = \frac{\varepsilon_{cu}}{c_u} - \frac{\varepsilon_{c,ps}}{c_{ps}} \tag{15}$$

where ϕ_{ps} is the curvature of RC column at the post-stressing stage and ϕ_u is the curvature of the RC column at the ultimate load stage.

Based on the assumption of curvature compatibility between the RC column and plates, the force P_{ptu} can be calculated by

$$P_{ptu} = \frac{1}{2} t_{pc} E_{pc} (h - c_{pu} + \frac{\varepsilon_{py}}{\phi}) \left[\varepsilon_{py} - (\varepsilon_{cu} - \varepsilon_{c,ps} + \varepsilon_{pc,ps} - h\phi) \right] \tag{16}$$

According to the proposed analytical model, the predicted axial load capacity (P_{pre}) of the specimens is determined by Eqs. (11) and (12). During the calculations of the ultimate load capacity of the RC columns, the extreme fiber compression strain of concrete ε_{cu} is assumed to be 0.003 (Park and Paulay 1975), and the gross sectional area of the concrete (A_c) does not include the areas of the bolt holes. The predicted axial load capacity of the specimens is presented in Table 3. Comparing the theoretical and experimental axial load capacities reveals that the proposed design procedure is generally able to conservatively estimate the actual axial load capacities of the plate-strengthened columns under eccentric compression loading with an average underestimation of 1%.

4. Strengthening of RC columns under large eccentric compression loading

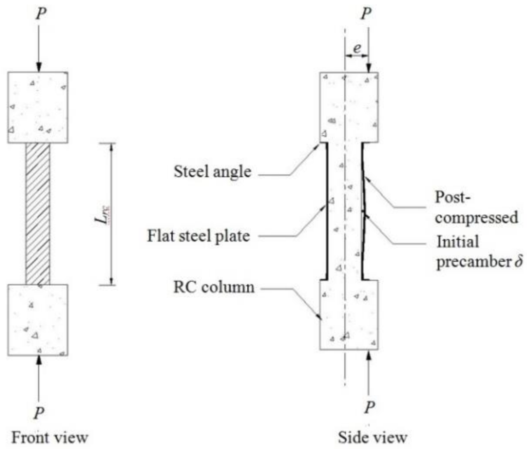

Fig. 8 The configuration of the column decompression approach

4.1 General

In this section, two post-compressed steel plates are placed on the side faces of RC column to strength the specimens, as shown in Fig. 8. The test results prove that the ultimate load capacity of the strengthened column is affected by the eccentricity, and the ultimate load capacity of the column is not improved significantly when the eccentricity is larger than that corresponding to the balance failure. It is because the de-compressive force generated by flattening post-compressed steel plates could significantly increase the tensile stress in the concrete core during the post-stressed stage under the large eccentric compression loading. The high tensile stress could accelerate the column failure. Hence, to address this shortcoming, the columns are still strengthened by post-compressed steel plates, but flat and post-compressed steel plates are placed respectively on the tension and compression sides of the RC column and decompression method is used on the compression side only.

In the experimental program, ten RC columns with different eccentricities, plate thicknesses and initial precamber displacements are tested under large eccentric compression loads. According to the eccentricity of the applied load, specimens are divided into three groups. In each group, one specimen without strengthening is acted as a control column, while the others are strengthened with flat and post-compressed steel plates. The axial strength, bending moment capacity, deformability and ductility of the strengthened RC columns are investigated.

4.2 Post stressed procedure

Su and Wang (2015) proposed a unified post-stress procedure is displayed in Fig. 9. The process can be divided into the following steps: (i) The compressed steel plate is fixed and bolts at the upper end of columns are tightened while the others are loosened before reaching the preloading level; (ii) The tensioned steel plate is installed and bolts at the both ends of columns are tightened when the specimen under preloading level, meanwhile the gaps between concrete and steel plates are filled with plaster until it

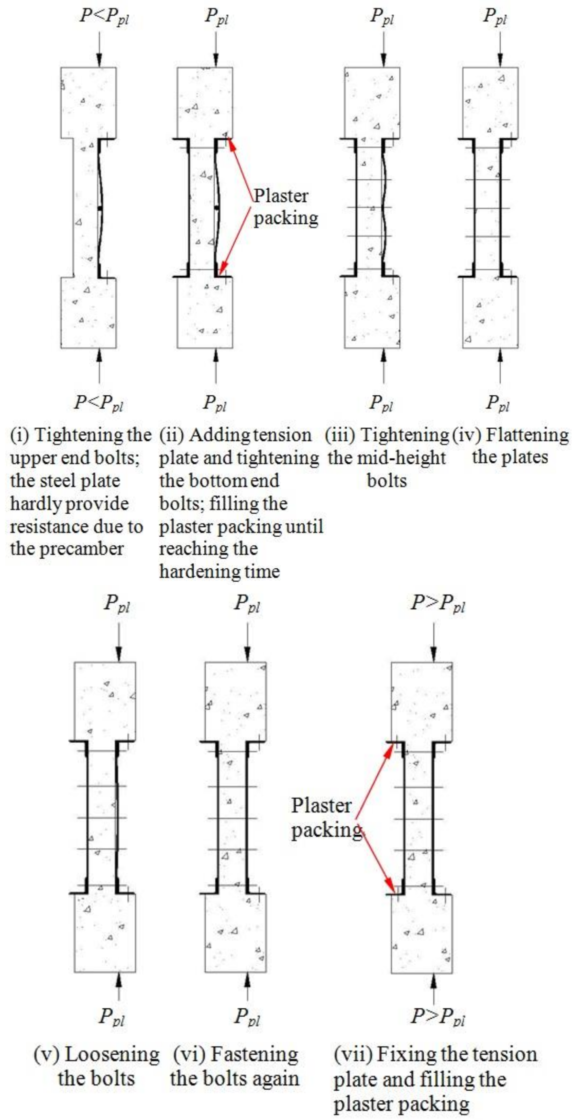

Fig. 9 Post-stressed procedure

reaches the hardening time; (iii) bolts at the mid-height are tightened, thus, the buckling mode of the post-compressed plate is changed to higher modes; (iv) the plates are flattened by tightening the rest of the bolts and (v & vi) to achieve a more evenly distributed internal stress in the plates, and all of the bolts are slightly loosened and fastened again; and (vii) The tension steel plate is fixed by bolts between steel angles and concrete and the gaps between steel angles and concrete are filled with plaster before increasing the loads.

4.3 Experimental observations

In the related experimental study, ten specimens are fabricated and tested. All specimens have the same dimensions with a clear column height (L_{rc}) of 600 mm and a uniform cross section of 150 mm × 100 mm. The 4T10 vertical steel bars are arranged, and a transverse reinforcement of R6 is adopted. All specimens are divided into three groups in accordance with the degrees of eccentricity (e). Specimens MSC1-1, MSC2-1 and MSC3-1

Table 4 Summary of strengthening details of specimens under large eccentric loading

Group	Specimen	f_{cu} (MPa)	f_c' (MPa)	e (mm)	t_{pt} (mm)	t_{pc} (mm)	δ (mm)	P_{pl} (kN)
A	MSC1-1	32.7	26.6	60	-	-	-	-
	MSC1-2	32.9	25	60	6	6	10	65
	MSC1-3	32.6	26.2	60	3	6	10	65
B	MSC2-1	29.7	24.2	100	-	-	-	-
	MSC2-2	29.5	24.4	100	3	3	10	43
	MSC2-3	29.5	24.4	100	6	6	6	43
	MSC2-4	30.1	24.7	100	6	6	10	43
	MSC2-5	31.6	25.2	100	3	6	10	43
C	MSC3-1	32.7	26.6	140	-	-	-	-
	MSC3-2	31.6	25.2	140	6	6	10	29

*t_{pt} = the thickness of a tension plate; t_{pc} = the thickness of a compression plate

Table 5 Summary of test results of specimens under large eccentric loading

Group	Specimen	λ	η	P_{exp} (kN)	P_{pre} (kN)	P_{pre}/P_{exp}
A	MSC1-1	1.27	1.6	218	213	0.98
	MSC1-2	1.32	1.99	389	381	0.98
	MSC1-3	1.49	1.71	360	368	1.02
B	MSC2-1	1.29	1.5	143	143	1
	MSC2-2	1.33	1.54	238	218	0.92
	MSC2-3	1.37	1.61	295	298	1.01
	MSC2-4	1.77	1.73	333	303	0.91
	MSC2-5	1.56	1.57	275	272	0.99
C	MSC3-1	1.11	1.36	89	97	1.09
	MSC3-2	1.21	1.53	234	223	0.95

are control columns without any strengthening measures to demonstrate the structural performance of RC columns prior to strengthening. The rest of specimens are strengthened by post-compressed steel plates with varying initial precamber and thickness of the tension (t_{pt}) and compression plate (t_{pc}). All strengthened columns are subjected to a preloading before the steel plate on the compression side is flattened, which is equal to 30% of the ultimate load capacity of the corresponding control column. For the strengthened columns, the axial load is applied under a force control with a loading rate of 2 kN per second. After tightening the bolts and flattening the post-compressed plate, the applied load is changed to a displacement control with a displacement rate of 0.5 mm per minute. The test is terminated when the post-peak load reaches 75% of the peak load. The design parameters, the preload and the compressive strength of the concrete cylinder (f_c') for all specimens are summarised in Table 4.

The concrete crack patterns and failure modes of the test specimens in each group are quite similar. For the specimens in Group A, the initial concrete cracks usually occur at the mid-height of the columns on the compression side and then propagate in the vertical direction. With an increasing applied load, the major cracks are extended and the concrete is spalled, as shown in Fig. 12(a). The failure mode is the crushing of concrete on the compression side, during which the tension reinforcements does not yield. For Group B and Group C, the initial concrete cracks usually occur at the mid-height of the columns on the tension side and then extend in the horizontal direction. As the applied load increased, the major cracks are extended, and vertical cracks are then formed on the compression side, as shown in Fig. 12(b). The failure mode is the yielding of tension steel followed by the crushing of concrete on the compression side. The ultimate axial load and moments are summarized in Table 5.

Compared with the control column in each of the groups, the strengthened specimens show various degrees of strengthening from 65.1% to 122.4%, which are summarized in Table 5. In Group A, the ultimate load capacity of Specimens MSC1-2 and MSC1-3 are increased by 78.4% and 65.1%. In Group B, the ultimate load capacities of Specimens MSC2-2, MSC2-3, MSC2-4 and MSC2-5 are enhanced by 66.4%, 106.3%, 122.4% and 88.8%, respectively. In Group C, the ultimate load capacity of Specimens MSC3-2 is increased by 121.4%.

The ultimate moment (M_u) at the mid-height of the column is composed of the primary moment (M_p) calculated based on the nominal eccentricity and the secondary moment (M_s) caused by the P-Δ effect. In Group A, the secondary moment of the strengthened columns MSC1-2 and MSC1-3 due to the P-Δ effect increase by 58.3% and 55.3%, respectively. In Group B, the secondary moment of the strengthened column due to the P-Δ effect increase by 97.2%, 239.3%, 237.2% and 159.3%. In Group C, the secondary moment of the strengthened column due to the P-Δ effect increase by 327.1%. It is evident that placing flat and post-compressed steel plates on the tension and compression sides respectively of the RC column and using decompression method on the compression side can significantly improve the ultimate axial and flexural capacities of RC columns under large eccentricity.

4.4 Deformation and ductility

The deformability factor (λ) and displacement ductility factor (η) can also be evaluated by Eqs. (9) and (10). The experimental results (Su and Wang 2015) demonstrate that the plate thickness plays an important role in increasing the deformability and ductility of the strengthened columns. But the effect of eccentricity of the applied load on the deformability and ductility is smaller than that of initial precamber and plate thickness.

4.5 Estimation of ultimate load capacity

The equilibrium equations can be obtained, respectively, from the sum of the internal forces and from taking moments about the tension steel, where f_{scy} is the yield strength of compression steel bars, f_{st} is the stress in the tension steel bars, t_{pt} is the thickness of the flattened steel plate, f_{pt} is the stress in the tension steel plate, A_{pt} is the cross-sectional area of the flattened steel plate, and h is the depth of the RC column; ε_{pc} is the strain

$$P_{pre} = \alpha\beta b c_u f_c^{'} + A_{sc} f_{scy} - A_{st} f_{st} + A_{pc} E_{pc} \varepsilon_{pc} - A_{pt} f_{pt} \quad (17)$$

$$P_{pre} e' = \alpha\beta b c_u f_c^{'} (d - \frac{\beta c_u}{2}) + A_{sc} f_{scy} (d - d^{'}) + A_{pc} E_{pc} \varepsilon_{pc} (d + \frac{t_{pc}}{2}) - A_{pt} f_{pt} (h - d + \frac{t_{pt}}{2}) \quad (18)$$

of post-compressed steel plate, which can be determined by (Su and Wang 2015)

$$\varepsilon_{pc} = \begin{cases} \varepsilon_{cu} - \varepsilon_{c,ps} + \varepsilon_{pc,ps} & (\varepsilon_{cu} - \varepsilon_{c,ps} + \varepsilon_{pc,ps} < \varepsilon_{pcy}) \\ \varepsilon_{pcy} & (\varepsilon_{cu} - \varepsilon_{c,ps} + \varepsilon_{pc,ps} \geq \varepsilon_{pcy}) \end{cases} \quad (19)$$

The stress in the tension steel bar (f_{st}) and tension steel plate (f_{pt}) can be calculated by

$$f_{st} = E_{st} \varepsilon_{scy} \frac{d - c_u}{c_u - d^{'}} \quad (20)$$

$$f_{pt} = E_{pt} (\varepsilon_{pcy} - \varepsilon_{pc,ps}) (\frac{h - c_u + \frac{t_{pt}}{2}}{c_u + \frac{t_{pc}}{2}}) \quad (21)$$

The depth of the compression zone (c_u) and ultimate load-carrying capacity (P_{pre}) are obtained from Eqs. (17) and (18). The de-compressive stress ($\varepsilon_{pc,ps}$) is controlled by the initial precamber of the steel plate. With the increase of the initial precamber, the de-compressive stress in the RC column is increased. If the occurrence of a reversed moment in the RC column is to be avoided, the magnitude of the de-compressive stress should satisfy Eq. (22). (Wang and Su 2013)

$$\delta \leq \frac{4}{\pi} \sqrt{ \frac{P_{pl} e' (\frac{c_{pl}}{\varepsilon_{c,pl}} - c_{pl}) \sin(\frac{L_{na}\varepsilon_{c,pl}}{2c_{pl}}) (\frac{c_{ps}}{\varepsilon_{c,ps}} - c_{ps}) \sin(\frac{L_{na}\varepsilon_{c,ps}}{2c_{ps}})}{P_{pl} e' - E_{pc} A_{pc} (\frac{t_{pc}}{2} + d)} - (\frac{c_{pl}}{\varepsilon_{c,pl}} - c_{pl})^2 \sin^2 (\frac{L_{na}\varepsilon_{c,pl}}{2c_{pl}}) } \quad (22)$$

The predicted axial load capacity (P_{pre}) of the specimens is presented in Table 5. During the calculations of the ultimate load capacity of the RC columns, the extreme fiber compression strain of concrete ε_{cu} is assumed to be 0.003 (Park and Paulay 1975). Comparing the theoretical and experimental axial load capacities reveals that the proposed theoretical model is generally able to conservatively estimate the actual axial load capacities of the plated-strengthened columns under eccentric compression loading with an average underestimation of 1%.

5. Repair of fire damaged RC columns with PCP

5.1 General

This section describes the axially loaded, fire-exposed, preloaded reinforced concrete columns strengthened with post-compressed steel plates. In the test program, seven RC columns with identical section dimensions and reinforcement details are fabricated and tested (Wang and Su 2014). Six of them are exposed to a four-hour fire load according to the ISO 834 Standard. Five of the fire-exposed columns are strengthened with post-compressed steel plates together with a post-compression method after one month of cooling. All columns are tested under axial compression to determine their ultimate load capacity, deformation and ductility.

The concrete temperature distribution is first presented and then a detailed evaluation of the strength, deformability and ductility performance of PCP strengthened columns are given. The effects of steel plate thickness, initial precamber displacements and preloading level on the ultimate load capacity of PCP strengthened columns are investigated. Finally, the internal force distribution between concrete and steel plates is reported and discussed in detail.

In the latter part of this section, an analytical model is described for the prediction of the ultimate axial load capacity of fire-exposed columns repaired with post-compressed steel plates. Comparison of the predicted and experimental results reveals that the analytical model can accurately predict the ultimate axial load capacity of the repaired columns.

Table 6 Summary of the material and geometry properties for repair works

Specimen	$f_{cu,s}$ (MPa)	$f_{c,s}^{'}$ (MPa)	$f_{cu,t}$ (MPa)	$f_{c,t}^{'}$ (MPa)	L_{rc} (mm)	t (min)	t_p (mm)	δ (mm)	P_{pl} (kN)
FSC1	53.2	48.3	54.1	48.8	850	-	-	-	-
FSC2	53.2	48.3	54.1	48.8	850	240	-	-	-
FSC3	52.4	46.5	52.8	46.7	850	240	8	10	640
FSC4	52.4	46.5	52.8	46.7	850	240	6	10	830
FSC5	54.2	47.8	54.7	47.8	850	240	6	6	640
FSC6	54.2	47.8	54.7	47.8	850	240	6	10	640
FSC7	54.9	46.3	54.9	46.3	850	240	6	14	640

*$f_{cu,s}$ = the concrete cube compression strength on the 28th day; $f_{c,s}^{'}$ = the concrete cylinder compression strength on the 28th day; $f_{cu,t}$ = the concrete cube compression strength on the fire test day; $f_{c,t}^{'}$ = the concrete cylinder compression strength on the fire test day

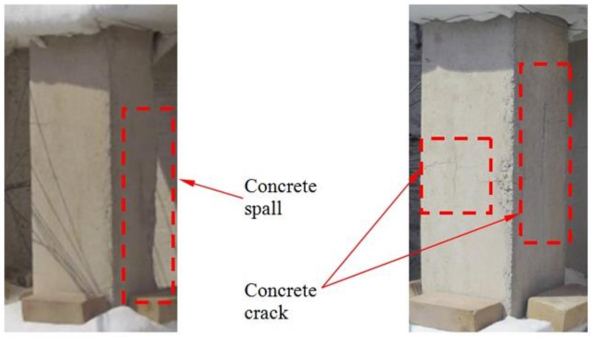

Fig. 10 Crack and spalls of specimens after the fire test

5.2 Specimens and test procedure

Seven specimens, namely FSC1 to FSC7, are fabricated and tested. The RC details of all specimens are identical. The RC cross sections are 300 mm × 250 mm, and the clear height of column is 850 mm. The vertical reinforcement of 6T12 is arranged, and transverse reinforcement of R6-80 is

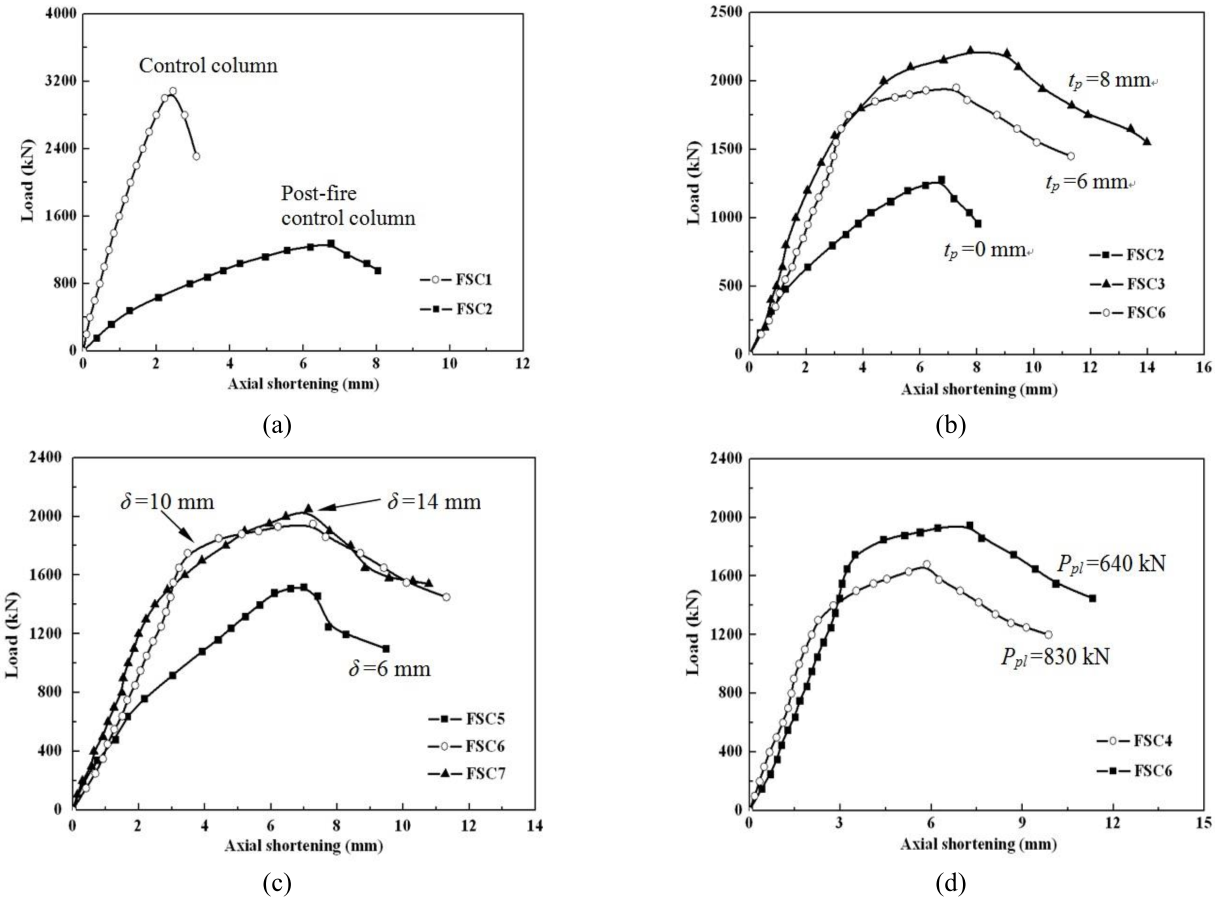

Fig. 11 Axial compression-shortening curves of specimens: (a) Effects of fire exposure; (b) Effects of plate thickness; (c) Effects of initial precamber and (d) Effects of preloading level

applied along the height of the column. All of the specimens have the same concrete cover of 40 mm. Specimen FSC1 is a control column with no strengthening measures or fire load, while Specimen FSC2 is a control column exposed to fire without any strengthening measures. They are used to demonstrate the structural performance of an RC column and a fire-exposed RC column prior to strengthening. The rest of the specimens are strengthened by post-compressed steel plates with a thickness (t_{pc}) of either 6 mm or 8 mm. The precamber at the middle height (δ) of columns varied from 6 mm to 14 mm. All of the strengthened columns are subjected to a preloading level (P_{pl}) before flattening the post-compressed steel plates, which range from 0.21 to 0.27 of the ultimate axial load capacities of Specimen FSC1. The design parameters for all specimens are summarized in Table 6.

The specimen is installed vertically in the furnace approximately one month after concrete casting. The fire procedure is under time control. After the specimen has been forced-air cooled to room temperature, the specimen is taken out of the furnace and stored in the laboratory for one month to ensure that the residual strength of the concrete would be minimized at the time of the axial load tests. To control the initial precamber of the steel plates, two stainless steel rods with a diameter equal to the initial precamber are inserted and fixed between the concrete and steel plates at the middle height of the column. The bolts at both ends of the column are then tightened to generate the designed initial precamber profile. The gaps between the steel angles and the concrete at the bottom and top of the steel plates are filled with an injection plaster, forming a layer of bedding between the steel angles and the concrete. The injection plaster is composed of plaster, potassium sulfate and water with a proportion of 37.5 : 1 : 15, by weight. To avoid local buckling of steel plates, the mortar is used to repair the spalled concrete before installing the steel plates. Fig. 10 shows the cracks and spalls of concrete after the fire test. When the applied compression reaches the preloading level, the post-stress procedure is adopted to avoid warping or buckling of steel plates during the decompression of the RC column by flattening the post-compressed steel plates. The test is terminated when the post-peak load reached 75% of the peak load.

5.3 Fire damaged evaluation

The experimental program was conducted by Wang and Su (2014). Compared with the post-fire control column (FSC2), the strengthened specimens show various degrees of strengthening from 18.9% to 74.0%, which are summarized in Table 7. The ultimate load capacities of Specimens FSC3, FSC4, FSC5, FSC6 and FSC7 are increased by 74.0%, 31.7%, 18.9%, 52.3% and 68.2%, respectively. Compared with the ultimate load capacity of the control column (FSC1), the ultimate load capacities of Specimens FSC3, FSC4, FSC5, FSC6 and FSC7 are restored up to 72.2%, 54.7%, 49.3%, 63.2% and 69.8%, respectively.

Fig. 11(a) shows the effects of fire on the ultimate load capacity of RC columns. Compared with the control column FSC1 (P_{exp}=3085 kN), the ultimate load capacity of Specimen FSC2 decrease by 58.5%. Fig. 11(b) shows the effects of the plate thickness (t_{pc}) on the ultimate load capacity (P_{exp}) under the same preloading level and initial precamber. Compared with Specimen FSC2 (t_{pc}=0 mm), the ultimate load capacities of Specimens FSC3 (t_{pc}=8 mm) and FSC6 (t_{pc}=6 mm) increase by 74.0% and 52.3%, respectively. Fig. 11(c) shows the effects of the initial precamber (δ) on the ultimate load capacity. The ultimate load capacity of Specimen FSC7 with δ = 14 mm is 2153 kN, which is 41.5% and 10.4% larger than the ultimate load capacities of Specimens FSC5 (δ=6 mm) and FSC6 (δ=10 mm), respectively. Because a larger initial precamber could generate a greater post-compressive force in the steel plates, a greater preloading in the original RC column could therefore be transferred to the steel plates. The reduction in the strain incompatibility between the steel plates and concrete enhances the ultimate load capacity of FSC7. Fig. 11(d) shows the effects of preloading level (P_{pl}) on the ultimate load capacity (P_{exp}). Compared with Specimen FSC6 (P_{pl}=640 kN), the ultimate load capacity of Specimen FSC4 (P_{pl}=830 kN) decrease by 15.7%. Therefore, the results clearly demonstrate that the use of thicker plates or increasing the initial precamber of plates can achieve a significantly higher ultimate load capacity.

5.4 Estimation of residual strength of concrete and steel bars and ultimate load capacity of repaired columns

Tan and Yao (2003) proposed the formulae to predict the residual strength of concrete (f_{cr}').

$$f_{cr}' = \beta_c \times f_c' \tag{23}$$

where f_c' is the cylinder compressive strength of concrete, and β_c is the strength reduction factor for concrete, which can be determined by Eq. (24) (Dotreppe *et al*. 1997).

$$\beta_c = \frac{\mu}{\sqrt{1+(0.3A_c^{-0.5}t_{ISO})^{A_c^{-0.25}}}} \tag{24}$$

in which A_c is the cross-sectional area of RC column in m^2, t_{ISO} is the ISO 834 fire exposure time in hours, and μ is the factor to account for spalling of concrete, which can be obtained by Eq. (25).

$$\mu = \begin{cases} 1-0.3t_{ISO} & (t_{ISO} \le 0.5\text{ hour}) \\ 0.85 & (t_{ISO} > 0.5\text{ hour}) \end{cases} \tag{25}$$

Lie (1992) proposed the formulae to predict the residual strength of steel bars (f_{sy}').

$$f_{sy}' = \begin{cases} f_{sy}[1.0+\dfrac{T}{900\ln(\frac{T}{1750})}] & (0 < T \le 600^\circ\text{C}) \\ f_{sy}(\dfrac{340-0.34T}{T-240}) & (600^\circ\text{C} < T < 1000^\circ\text{C}) \end{cases} \tag{26}$$

where f_{sy} is the yield strength of steel reinforcement, and T is the temperature of steel bar.

The ultimate axial load capacity (P_{pre}) of the plate-repaired column is expressed as (Su and Wang 2012)

$$P_{pre} = 0.85A_c f_{cr}' + A_s f_{sy}' + 2\gamma A_p f_{py} \tag{27}$$

where A_s and A_p are the cross-sectional areas of longitudinal reinforcement and steel plates respectively, f_{py} is the yield strength of steel plates, and γ is the plate strength utilisation coefficient.

The predicted axial load capacity (P_{pre}) of the specimens is presented in Table 7. During the calculations of the ultimate load capacity of RC columns, the strain of concrete ε_{co} corresponding to the peak load was assumed to be 0.002. Comparing the theoretical and experimental axial load capacities reveals that this theoretical model is generally able to conservatively estimate the actual axial load capacities of fire-exposed RC columns strengthened with post-compressed steel plates with an average overestimation of 8%.

Table 7 Summary of deformability and ductility factors, axial load capacities and predicted values of fire-exposed specimens

Specimen	λ	η	P_{exp} (kN)	P_{pre} (kN)	P_{exp} / P_{pre}
FSC1	1.12	1.09	3085	3020	1.02
FSC2	1.19	1.42	1280	1012	1.26
FSC3	1.73	2.21	2227	1911	1.17
FSC4	1.56	2.11	1686	1479	1.14
FSC5	1.34	1.73	1522	1490	1.02
FSC6	1.55	2.09	1950	1738	1.12
FSC7	1.51	2.10	2153	1913	1.13

5.5 Fire resistance requirements for repaired columns

Because of the use of steel plates, fire protection of the structural steel should be a concern. A common fire protection for steel plates by intumescent flame-retardant coating could be used. The initial thickness of the intumescent coating (d_c) can be determined by Eq. (28) (Li *et al*. 2012).

$$d_c = \mathrm{R}_{eq}\, \lambda_{ef}\, f \tag{28}$$

where R_{eq} and λ_{eff} are the equivalent thermal resistance and the effective thermal conductivity, respectively, which can be calculated by Eqs. (29) and (30) according to standard DD ENV 13381-4 (British Standards Institution (BSI) 2002).

$$\mathrm{R}_{eq} = \frac{\left[T_g(t)-T_s(t)\right]A_i}{(\Delta T_s/\Delta_t)C_s\rho_s V} \tag{29}$$

$$\lambda_{eff} = \Delta T_s e^{\phi/10}\left[\frac{dcC_s\rho_s(1+\phi/3)}{A_i V(T_g(t)-T_s(t))\Delta_t}\right] \tag{30}$$

where t is the fire exposure time; $T_g(t)$ and $T_s(t)$ are the temperatures of the fire and the surface between insulation and steel, respectively; A_i is the appropriate area of the fire insulation material per unit length; V is the volume of the steel per unit length; Δ_t is the time increment; $C_s\rho_s$ is the volumetric specific heat of the steel; ΔT_s is the steel temperature increment; and ϕ is the mass ratio of intumescent coating.

6. Conclusions

This paper summarized the studies related to the behavior of preloaded RC columns strengthened with PCP. Based on the information presented, the following concluding remarks are made:

• To address the effects of pre-existing loads on stress-lagging between the concrete core and the new jacket, PCP strengthening technique is introduced. The comprehensive experimental and analytical studies on strengthened RC columns under axial compressive loading were carried out. The effects of initial precamber displacement, steel plate thickness and preloading level on the ultimate load capacity of strengthened columns were investigated. In the meantime, the experimental results prove that the PCP strengthening technique is an effective method to recover the ultimate load capacity of the fire-exposed RC columns.

• The test results indicated that thicker steel plates and larger initial precamber can improve the ultimate load capacity of RC columns, and larger plate thickness can also enhance the axial deformation capacity of RC columns significantly. In the meantime, the steel plates with larger initial precamber can share much more existing axial load in the original concrete column, hence the stress-lagging effect can be alleviated. Moreover, external steel plates can considerably increase the ductility of the strengthened columns under axial compression loading. The prediction of the ultimate load capacity of PCP strengthened RC columns with consideration of stress-lagging effects would underestimate the capacity by 7%.

• The experimental results show that the ultimate load capacity of PCP strengthened RC columns under eccentric compressive loading is affected by the initial precamber displacement, plate thickness and degree of eccentricity, especially the last one. If the eccentricity is less than that corresponding to the balance failure, the higher ultimate load capacity of the strengthened columns can be obtained when the post compressed steel plates are placed on the side faces of RC columns; if the eccentricity is larger than that corresponding to the balance failure, placing flat and post compressed steel plates on the tension and compression sides of the RC column respectively and using the decompression method on the compression side only is more effective to improve the ultimate load capacity of strengthened columns.

• Although the ultimate axial load capacity of RC columns after four hours fire exposure decrease sharply, the use of PCP strengthening technique to repair them can restore up to 72% of the original ultimate load level. The experimental results show that PCP can actively share the existing axial load in the original column. Stress-lagging effects can be alleviated by controlling the initial post-compressed profile of the steel plates. External steel plates can considerably enhance the axial strength and the deformation capacity of the plate-strengthened columns under axial compression loading. Thicker steel plates and a larger initial precamber can enhance the ultimate load capacity of columns.

Acknowledgments

The research described here was supported by the National Natural Science Foundation of China (Grant No. 51678297), Natural Science Foundation of Jiangsu Province (Grant No. BK20140946) and National Natural Science Foundation for the Youth of China (Grant No. 51408305).

References

Achillopoulou, D.V. and Karabinis, A.I. (2013), "Investigation of shear transfer mechanisms in repaired damaged concrete columns strengthened with RC jackets", *Struct. Eng. Mech.*, **47**(4), 575-598.

British Standards Institution (BSI) (2002), *Test Methods for Determining the Contribution to the Fire Resistance of Structural Members-Part 4: Applied Protection to Steel Members*, DD ENV 13381-4, London, U.K.

Cirtek, L. (2001), "RC columns strengthened with bandage-experimental programme and design recommendations", *Constr. Build. Mater.*, **15**(8), 341-349.

Dotreppe, J.C., Franssen, J.M., Bruls, A., Baus, R., Vandevelde, P., Minne, R., Van Nieuwenburg, D. and Lambotte, H. (1997), "Experimental research on the determination of the main parameters affecting the behavior of reinforced concrete columns under fire conditions", *Mag. Concrete Res.*, **49**(179), 117-127.

Elwan, S.K. and Rashed, A.S. (2011), "Experimental behavior of eccentrically loaded R.C. short columns strengthened using GFRP wrapping", *Struct. Eng. Mech.*, **39**(2), 207-221.

Ersoy, U., Suleiman, R. and Tankut, T. (1993), "Behavior of jacketed columns", *ACI Struct. J.*, **90**(3), 288-293.

Frangou, M., Pilakoutas, K. and Dritsos, S. (1995), "Structural repair/strengthening of RC columns", *Constr. Build. Mater.*, **9**(5), 259-266.

Fukuyama, H. and Sugano, S. (2000), "Japanese seismic rehabilitation of concrete buildings after the Hyogoken-Nanbu earthquake", *Cement Concrete Compos.*, **22**(1), 59-79.

Giménez, E., Adam, J.M., Ivorra, S. and Calderón, P.A. (2009a), "Influence of strips configuration on the behaviour of axially loaded RC columns strengthened by steel caging and strips", *Mater. Des.*, **30**(10), 4103-4111.

Giménez, E., Adam, J.M., Ivorra, S., Moragues, J.J. and Calderón, P.A. (2009b), "Full-scale testing of axially loaded RC columns strengthened by steel angles and strips", *Adv. Struct. Eng.*, **12**(2), 169-181.

Harajli, M.H., Hantouche, E. and Soudki, K. (2006), "Stress-strain model for fiber-reinforced polymer jacketed concrete columns", *ACI Struct. J.*, **103**(5), 672-680.

Kong, F.K. and Evans, R.H. (1987), *Reinforced and Prestressed Concrete*, Van Nostrand Reinhold (International).

Kumar, V. and Patel, P.V. (2016), "Strengthening of axially loaded concrete columns using stainless steel wire mesh (SSWM)-numerical investigations", *Struct. Eng. Mech.*, **60**(6), 979-999.

Li, G.Q., Lou, G.B., Zhang, C., Wang, L.L. and Wang, Y.C. (2012), "Assess the fire resistance of intumescent coatings by equivalent constant thermal resistance", *Fire Technol*., **48**(2), 529-546.

Lie, T.T. (1992), *Structural Fire Protection*, ASCE Manuals and Rep. on Engineering Practice No. 78, ASCE, New York, U.S.A.

Montuori, R. and Piluso, V. (2009), "Reinforced concrete columns strengthened with angles and battens subjected to eccentric load", *Eng*. *Struct*., **31**(2), 539-550.

Park, R. and Paulay, T. (1975), *Reinforced Concrete Structures*, John Wiley & Sons publications.

Pellegrino, C. and Modena, C. (2010), "Analytical model for FRP confinement of concrete columns with and without internal steel reinforcement", *J*. *Compos*. *Constr*., **14**(6), 693-705.

Ramirez, J.L. (1996), "Ten concrete column repair methods", *Constr*. *Build*. *Mater.*, **10**(3), 195-202.

Su, R.K.L. and Wang, L. (2009), "Compressed plates for strengthening preloaded rectangular reinforced concrete columns", *Proceedings of the 7th International Conference on Tall Buildings*, Hong Kong, China, October.

Su, R.K.L. and Wang, L. (2012), "Axial strengthening of preloaded rectangular concrete columns by precambered steel plates", *Eng*. *Struct*., **38**, 42-52.

Su, R.K.L. and Wang, L. (2015), "Flexural and axial strengthening of preloaded concrete columns under large eccentric loads by flat and precambered steel plates", *Struct*. *Infrastruct*. *E*., **11**(8), 1083-1101.

Takeuti, R.A., De Hanai, J.B. and Mirmiran, A. (2008), "Preloaded RC columns strengthened with high-strength concrete jackets under uniaxial compression", *Mater*. *Struct*., **41**(7), 1251-1262.

Teng, J.G., Chen, J.F., Smith, S.T. and Lam, L. (2003), "Behaviour and strength of FRP-strengthened RC structures: A state-of-the-art review", *Struct*. *Bulid*., **156**(1), 51-62.

Timoshenko, S.P. and Gere, J.M. (1961), *Theory of Elastic Stability*, McGraw-Hill.

Wang, L. (2013), "Post-compressed plates for strengthening preloaded reinforced concrete columns", Ph.D. Dissertation, The University of Hong Kong, China.

Wang, L. and Su, R.K.L. (2013), "A unified design procedure for preloaded rectangular RC columns strengthened with post-compressed plates", *Adv*. *Concrete Constr*., **1**(2), 165-187.

Wang, L. and Su, R.K.L. (2014), "Repair of fire-exposed preloaded rectangular concrete columns by post compressed steel plates", *J*. *Struct*. *Eng*., **140**, 329-340.

Wu, Y.F., Liu, T. and Oehlers, D.J. (2006), "Fundamental principles that govern retrofitting of reinforced concrete columns by steel and FRP jacketing", *Adv*. *Struct*. *Eng*., **9**(4), 507-533.

Wu, Y.F. and Wei, Y.Y. (2010), "Effect of cross-sectional aspect ratio on the strength of CFRP confined rectangular concrete columns", *Eng*. *Struct*., **32**(1), 32-45.

Yuce, S.Z., Yuksel, E., Bingol, Y., Taskin, K., Karadogan, H.F. (2007), "Local thin jacketing for the retrofitting of reinforced concrete columns", *Struct*. *Eng*. *Mech*., **27**(5), 589-607.

Zhang, B., Yang, Y., Wei, Y.F., Liu, R.Y., Ding, C. and Zhang, K.Q. (2015), "Experimental study on seismic behavior of reinforced concrete column retrofitted with prestressed steel strips", *Struct*. *Eng*. *Mech*., **55**(6), 1139-1155.

CC